Bioconjugate Chemistry

Article

pubs.acs.org/bc

Development of Injectable Hyaluronic Acid/Cellulose Nanocrystals Bionanocomposite Hydrogels for Tissue Engineering Applications

This paper was originally submitted for the "Biofunctional Biomaterials: The Third Generation of Medical Devices", published as the July 15, 2015, issue of Bioconjugate Chemistry (Vol. 26, No. 7).

Rui M. A. Domingues,[†,‡] Marta Silva,[†,‡] Pavel Gershovich,[†,‡] Sefano Betta,[§,∥] Pedro Babo,[†,‡] Sofia G. Caridade,[†,‡] João F. Mano,[†,‡] Antonella Motta,[§,∥] Rui L. Reis,[†,‡] and Manuela E. Gomes*[,†,‡]

[†]3B's Research Group - Biomaterials, Biodegradables and Biomimetics, Department of Polymer Engineering, University of Minho, Headquarters of the European Institute of Excellence on Tissue Engineering and Regenerative Medicine, Avepark − Parque de Ciência e Tecnologia, Zona Industrial da Gandra, 4805-017 Barco, Guimarães, Portugal

[‡]ICVS/3B's-PT Associated Laboratory, 4805-017 Braga/Guimarães, Portugal

[§]Department of Industrial Engineering and Biotech Research Centre, University of Trento, 38123 Trento, Italy

[∥]European Institute of Excellence on Tissue Engineering and Regenerative Medicine, 38123 Trento, Italy

Supporting Information

ABSTRACT: Injectable hyaluronic acid (HA)-based hydrogels compose a promising class of materials for tissue engineering and regenerative medicine applications. However, their limited mechanical properties restrict the potential range of application. In this study, cellulose nanocrystals (CNCs) were employed as nanofillers in a fully biobased strategy for the production of reinforced HA nanocomposite hydrogels. Herein we report the development of a new class of injectable hydrogels composed of adipic acid dihydrazide-modified HA (ADH-HA) and aldehyde-modified HA (a-HA) reinforced with varying contents of aldehyde-modified CNCs (a-CNCs). The obtained hydrogels were characterized in terms of internal morphology, mechanical properties, swelling, and degradation behavior in the presence of hyaluronidase. Our findings suggest that the incorporation of a-CNCs in the hydrogel resulted in a more organized and compact network structure and led to stiffer hydrogels (maximum storage modulus, E', of 152.4 kPa for 0.25 wt % a-CNCs content) with improvements of E' up to 135% in comparison to unfilled hydrogels. In general, increased amounts of a-CNCs led to lower equilibrium swelling ratios and higher resistance to degradation. The biological performance of the developed nanocomposites was assessed toward human adipose derived stem cells (hASCs). HA-CNCs nanocomposite hydrogels exhibited preferential cell supportive properties in in vitro culture conditions due to higher structural integrity and potential interaction of microenvironmental cues with CNC's sulfate groups. hASCs encapsulated in HA-CNCs hydrogels demonstrated the ability to spread within the volume of gels and exhibited pronounced proliferative activity. Together, these results demonstrate that the proposed strategy is a valuable toolbox for fine-tuning the structural, biomechanical, and biochemical properties of injectable HA hydrogels, expanding their potential range of application in the biomedical field.

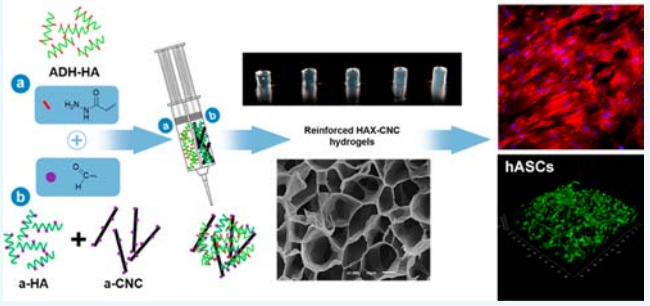

INTRODUCTION

Hyaluronic acid (HA) is a high-molecular-mass linear polysaccharide of alternating D-glucuronic acid and *N*-acetyl-D-glucosamine, ubiquitously found in tissues and body fluids of vertebrates and some bacteria.[1−3] It is a crucial component of the natural extracellular matrix having an important role in several cellular and tissue functions.[4] HA presents unique properties such as good biocompatibility, gel-forming properties, and ability to be easily modified through both its carboxyl and hydroxyl groups, which potentiate its use in tissue engineering (TE) and regenerative medicine as a starting material for the production of hydrogels.[5,6] Moreover, it is naturally degraded by hyaluronidases (HAses), which hydrolyze the hexosaminidic $\beta(1 \rightarrow 4)$ linkages between *N*-acetyl D-glucosamine and D-glucuronic acid residues. Since the degradation rate of HA, mediated by HAses, can be increased in case of injury, HA-based materials have the advantage to be degraded and release their content in a controlled manner.[2,7] Recent studies have been focusing on the development of HA-based injectable hydrogels, which can be formed in situ after being injected into the body.[6,8,9] The main advantages of this approach rely on the ability of injectable hydrogels to adapt to

Received: April 15, 2015
Revised: June 22, 2015
Published: June 24, 2015

DOI: 10.1021/acs.bioconjchem.5b00209
Bioconjugate Chem. 2015, 26, 1571−1581

the defect shape and to be easily laden with cells and/or drugs. Additionally, its delivery is performed through minimally invasive surgical procedures, resulting in a faster recovery, reduced scarring, and less pain for patients.[10] Chemically cross-linked HA-based hydrogels can be obtained through a variety of chemistries, such as Schiff's base, enzyme-mediated, photopolymerization, Michael-type addition, disulfide formation, and several click chemistry reactions.[6,11−13] Specifically, the hydrazone bond click reaction between hydrazide and aldehyde groups has been widely used for the preparation of natural polymer based hydrogels.[14−16] Moreover, it has been previously demonstrated for several polymeric systems that hydrazone cross-links are formed when the functionalized hydrogel components come into contact under normal physiological conditions and does not pose considerable cytotoxicity issues.[17−19] Despite the above-mentioned features that make the HA an appealing precursor for the development of biomaterials for tissue engineering applications, HA as well as other natural polymer-based hydrogels have limited mechanical properties and degradation rates, restraining their clinical applications.[12,20] Biomaterials used in tissue engineering applications, besides providing specific biological cues, should create an adequate mechanical environment to support cell migration, proliferation, and differentiation aiming at regeneration of functional tissues.[10,21] Moreover, they must maintain suitable mechanical features during new tissue formation without deformation or collapse.[21,22]

In order to improve the mechanical properties and control the degradability of HA-based hydrogels, HA can be chemically modified or physically cross-linked.[15,23] Additional strategies consist of the reinforcement of hydrogels with nanoparticles, such as natural based cellulose nanocrystals (CNCs), resulting in a composite material with improved mechanical properties.[19] CNCs can be extracted from a wide range of highly available cellulose sources following well established chemical routes.[24] Along with the general good biocompatibility, CNCs present high strength (elastic modulus ranging from 110 to 220 GPa and tensile strength is in the range of 7.5−7.7 GPa[25−29]), low density, high aspect ratio, and surface area that greatly contribute to their potential use in regenerative medicine and TE applications.[30] Moreover, its surface chemistry enables different specific surface modifications, such as oxidation, esterification, etherification, silylation, or polymer grafting, which allow the effective incorporation of CNCs into the hydrogel matrices, where it can act as both filler and cross-linker.[30,31] Another interesting aspect of CNCs obtained from the typical sulfuric acid hydrolysis for potential TE applications is the presence of abundant surface SO_3^- half-ester groups. This feature may also confer additional interesting functional properties to the hydrogels, as this functionality is also characteristic of the ECM sulfated glycosaminoglycans which are known to induce and control specific cell functions on the cellular microenvironment.[32]

In this work we developed injectable hydrogels based on the hydrazone covalent cross-linking reaction, composed of adipic acid dihydrazide-modified HA (ADH-HA) and aldehyde-modified HA (a-HA) reinforced with varying contents of aldehyde-modified CNCs (a-CNCs) (Figure 1). The hydrogel precursors and cross-linked hydrogels were thoroughly characterized regarding their chemical, morphological, microstructural, and mechanical properties, as well as their swelling and degradation profiles.

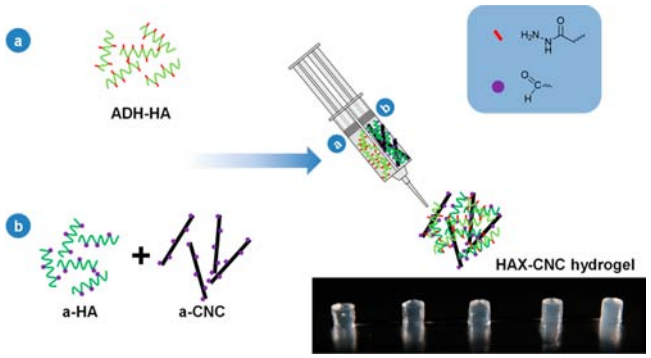

Figure 1. Schematic representation of the proposed injectable hyaluronic acid-based hydrogels (HAX) reinforced with CNCs, prepared using a double barrel syringe. (a) Hydrazide-functionalized hyaluronic acid (ADH-HA) and (b) aldehyde functionalized hyaluronic acid (a-HA), with or without aldehyde-modified CNCs (a-CNCs), will be coinjected and mixed. Stable hydrogels will be formed upon cross-link reaction between the hydrazide and carbonyl moieties of precursor components.

RESULTS AND DISCUSSION

Chemical and Morphological Characterization of HAX and HAX-CNC. Considering their unique mechanical properties, CNCs have been incorporated as fillers in several polymeric hydrogel matrices, such as for example to improve the thermal and mechanical properties of gelatin based hydrogels[33] or to improve the stability and the mechanical properties of poly(vinyl alcohol)[34,35] or α-cyclodextrin[36] hydrogels. However, only a few studies explored the possibility of using CNCs not only as fillers (i.e., with no covalent attachment to the hydrogel matrix), but also as cross-linker agents, a strategy that usually results in enhanced mechanical properties when compared with the mere physical entrapment of the CNCs within the hydrogel matrix.[19,33] To be used as cross-linkers, chemical functionalization of their surfaces is usually required. In this work, CNCs were functionalized following the well-described[33,37] sodium periodate oxidation route that induces the cleavage of the C2—C3 glycol bond of glucose residues, leading to the formation of dialdehyde groups at the respective carbon atoms along the cellulose chains.

The reactive aldehyde groups are particularly appealing for a wide range of biomedical applications due to their ability to spontaneously react with amine groups in a Schiff base reaction or condense with hydrazide groups to form covalent hydrazone linkages. The latter chemical route was used to synthesize injectable covalently cross-linked hydrogels by in situ hydrazone formation between adipic acid dihydrazide modified hyaluronic acid (ADH-HA) and aldehyde modified HA (a-HA). Thus, aldehyde modified CNCs (a-CNCs, Figure S2) are expected to participate in the cross-linked polymeric network resulting in HAX-CNC nanocomposite hydrogel with enhanced mechanical and structural performance.

Injectable and covalently cross-linked hyaluronic acid hydrogels (HAX) reinforced with a-CNCs were produced by the coinjection of the precursor components using a commercial double barrel syringe (Figure 1). In general, all the hydrogel formulations formed quickly upon contact of the two HA derivatives and the a-CNCs (see Movie in Supporting Information), a characteristic of several hydrazone cross-linked HA hydrogels which present typical gelation times within 3 to 30 s.[19,38,39] The incorporation of a-CNC did not have a

DOI: 10.1021/acs.bioconjchem.5b00209
Bioconjugate Chem. 2015, 26, 1571−1581

significant impact on the apparent gelation time of the hydrogels, which were in the range of 15 ± 0.3 to 17 ± 1 s.

Successful cross-linking of the hydrazide-functionalized HA with the aldehyde moieties of the a-HA or a-CNC was confirmed by FTIR. Overall the spectra of the hydrogel precursor components and the HAX-CNC showed similar patterns (Figure 2). In the spectrum of HA-ADH, the main differences compared to that of HA are the appearance of the characteristic peaks of the ADH-modification at 1710 (only seen as a slight slop), 1550, and 1375 cm^{-1} (stronger than in the nonmodified HA), while in the spectrum of a-HA it is possible to observe the carbonyl stretch band at around 1735 cm^{-1}, similarly to a-CNC. In the HAX-CNC hydrogels, the band of the carbonyls that are consumed in the covalent hydrazone cross-linking reaction disappears, confirming the covalent cross-linking between the hydrogel components.

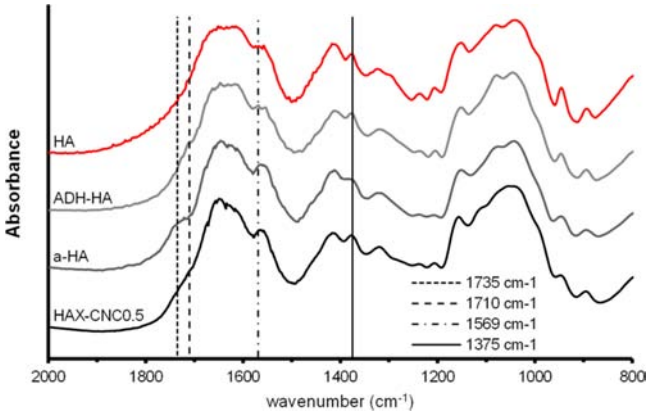

Figure 2. FTIR transmittance spectra of hyaluronic acid (HA), hydrazide modified hyaluronic acid (ADH-HA), aldehyde functionalized hyaluronic acid (a-HA), and HA hydrogel containing 0.5 wt % of a-CNCs (HAX-CNC 0.5%). The dashed lines signal the peaks corresponding to the CH_2 deformation, vibrational bending at ~1375 cm^{-1}, amide II (R—C═O—NH—R′) NH bending at ~1569 cm^{-1}, and carbonyl stretch at ~1710 cm^{-1}; and anhydrous aldehyde (R—C═O) stretch at ~1735 cm^{-1}.

The morphology of the HAX hydrogels and the influence of a-CNC incorporation on their microstructure were investigated by scanning electron microscopy (SEM). Cross sections of the HAX hydrogel formulations were produced by fracturing freeze-dried hydrogels after immersion in liquid nitrogen. Representative images of the cross sections analyzed by SEM are depicted in Figure 3.

The HAX-CNC 0% hydrogels present a disorganized interconnected porous structure with an average pore size around 37 μm (Figure 3Aa), similar to what is commonly observed in freeze-dried hydrogels.[13,33] The incorporation of CNCs resulted in a relatively organized and compact structure, with significantly smaller pores ranging from 19.6 to 29.5 μm for HAX-CNC 0.125% and HAX-CNC 0.5%, respectively (Figure 3B). Dash and co-workers reported a similar effect after covalent cross-linking a-CNCs within gelatin hydrogels.[33] This effect was ascribed to the increased cross-linking density resulting from the incorporation of the aldehyde-functionalized nanofiller. Nevertheless, the pore sizes tend to increase among the HAX-CNC formulations, proportionally with the incorporation of increasing ratios of a-CNCs (Figure 3B). This phenomenon may be related to two aspects. On one hand, higher amounts of a-CNCs will increase the hydrogen bonding density between the stiff nanofiller and the polymer matrix restricting chain backbone motion. On the other hand, both nanofiller and polymer matrix are negatively charged which may result in a steric-blocking mechanism also restricting the chain mobility. These combined effects may result in reduced covalent cross-linking between polymeric precursors, thus explaining the increased pore sizes observed at higher a-CNC loading.

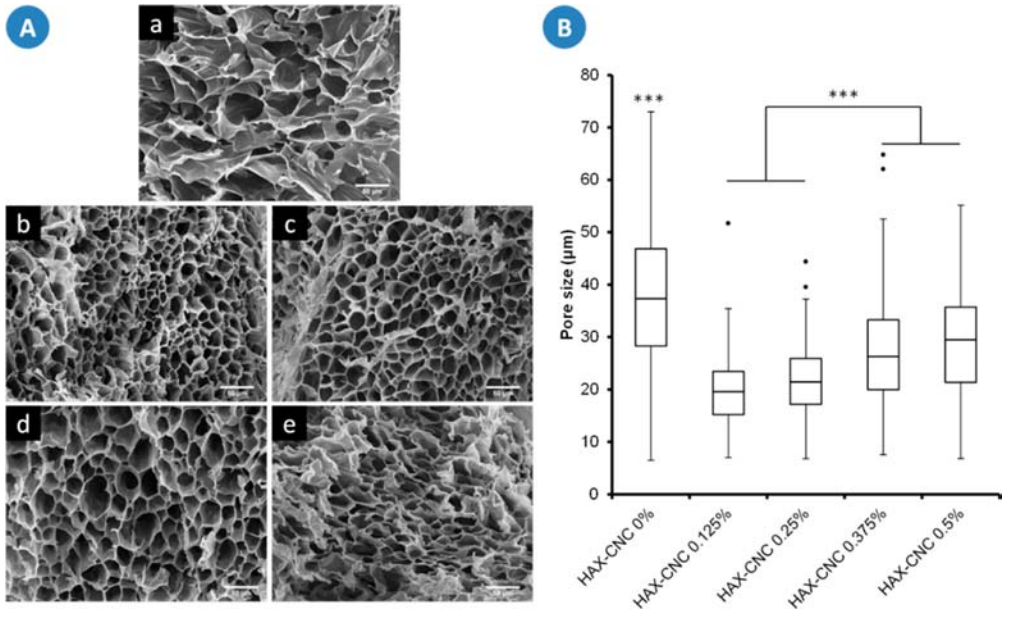

Figure 3. (A) Cross-sectional SEM pictures of the hydrogel formulations: (a) HAX-CNC 0%; (b) HAX-CNC 0.125%; (c) HAX-CNC 0.25%; (d) HAX-CNC 0.375%; (e) HAX-CNC 0.5%. Magnification 300× (scale bar 50 μm). (B) Box-plot representation of the pore size distribution in the formulations HAX, HAX-CNC 0.125%, HAX-CNC 0.25%, HAX-CNC 0.375%, and HAX-CNC 0.5%. $N > 50$; three symbols $p < 0.001$ by One-Way ANOVA followed by Tukey posthoc test for multiple comparisons.

DOI: 10.1021/acs.bioconjchem.5b00209
Bioconjugate Chem. 2015, 26, 1571−1581

Mechanical Properties of HAX and HAX-CNC Hydrogels. The mechanical/viscoelastic properties of the hydrogels were tested in dynamic and simulated human physiological conditions by dynamical mechanical analysis (DMA). The results are presented in Figure 4 where the storage modulus

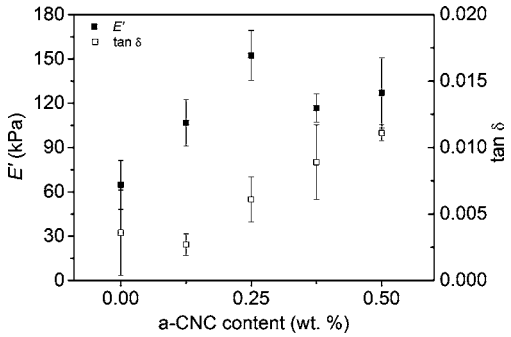

Figure 4. Storage modulus (E') and loss factor (tan δ) of the HA hydrogels with various a-CNC contents measured at 1 Hz with the samples immersed in PBS at room temperature (RT).

(E') and the loss factor (tan δ) of all the groups at the frequency of 1 Hz are shown. Overall, the incorporation of a-CNCs in the HA matrix lead to stiffer hydrogels indicating that they induce a reinforcement effect by acting as effective junction elements. Hydrogels reinforced with a-CNCs, exhibited E' and tan δ values that ranged between 107 and 152 kPa and 0.003−0.01, respectively. In comparison to the hydrogels without a-CNCs, E' increased by 65% and 135% for a-CNCs content 0.125 and 0.25 wt %, respectively. Nonetheless, the formulations with higher amounts of a-CNCs (0.375 and 0.5 wt %) did not follow this trend. Above a critical amount of 0.25 wt %, E' decreased, although still being higher (80% and 96%, respectively) than HAX-CNC 0% hydrogels. This occurrence is in line with the results from previous reports[19] and may be explained by the occurrence of a steric-blocking mechanism at higher amounts of CNCs, restricting the polymer chain mobility and cross-linking, as previously discussed. In fact, this observation can be correlated with the pore size distribution of the hydrogels as observed by SEM (Figure 3) in which all the HAX-CNC hydrogel formulations exhibited smaller pore size than unfilled HAX, while a significant increase was observed between HAX-CNC (0.125−0.25%) and HAX-CNC (0.375−0.5%).

The tan δ is the ratio of the amount of energy dissipated by viscous mechanisms relative to energy stored in the elastic component providing information about the damping properties of the material. The hydrogels exhibited an increasing trend of tan δ with the increase of CNC contents in the hydrogels. Nonetheless, the very low values (near zero) are indicative of the highly elastic properties of these hydrogels and low energy dissipating potential.

Comparison between the results obtained in this study and the ones described in the literature is challenging since the hydrogel mechanical properties strongly depend on the physicochemical characteristics of the precursor polymers as well as cross-linking chemistry, and also because most of the studies choose to assess it based on rheology analysis. Nevertheless, taking as a reference other studies where a-CNCs have been employed for the reinforcement of naturally based polymer hydrogels, some comparisons may be devised. Previous studies on the reinforcement of dextran-carboxymethyl cellulose hydrogels with a-CNCs, prepared in a very similar way to HAX-CNCs, reported a maximum G' of 6.7 kPa for a nanofiller content of 0.375 wt %, representing an improvement of 140% compared to unfilled hydrogels.[19] Dash et al. also reported a G' improvement of 150% in gelatin hydrogels cross-linked with a-CNCs (around 13 wt % relatively to the gelatin matrix) compared to unfilled hydrogels. In the present study, HAX-CNCs hydrogels exhibit improvements of the maximum storage modulus of the same order (135% for 0.25 wt % a-CNC content). Moreover, both works also reported low tan δ values, characteristic of elastic networks. Thus, according to our results, the incorporation of variable amounts of a-CNCs into the HA matrix may be a useful tool for tuning the hydrogel mechanical properties, expanding the range of potential applications of HA-based hydrogels in tissue engineering strategies.

From this perspective, it is well-known that, generally, cells tend to adhere more strongly to stiffer materials than on softer ones, and increasing evidence suggests that the stiffness of the scaffolds is sensed by mesenchymal stem cells, which may undergo phenotypic lineage differentiation depending on the matrix elasticity through mechanotransduction mechanisms.[40]

Swelling and Degradation. The swelling properties of the hydrogels were monitored as a function of incubation time in PBS at 37 °C (Figure 5). Overall, the swelling ratio positively correlated with the immersion time of all samples which presented a similar swelling profile during the first 3 days of immersion. After 3 days of incubation, swelling induced a maximum mass increase of 54 ± 2.3% in HAX-CNC 0.5%

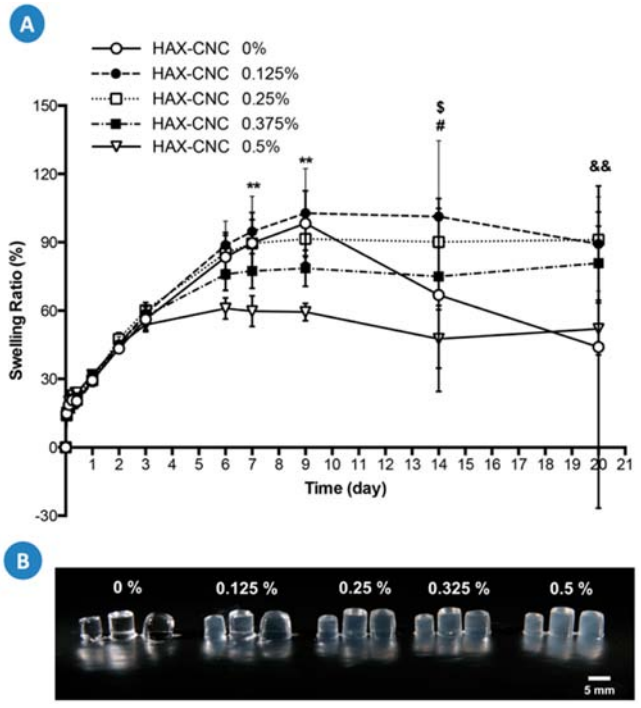

Figure 5. (A) Swelling profile of the hydrogels in PBS at 37 °C. * HAX-CNCs 0.5% vs HAX-CNCs (0−0.25%), # HAX-CNCs 0.5% vs HAX-CNCs (0.125−0.375%), $ HAX-CNCs 0% vs HAX-CNCs (0.125−0.25%); & HAX-CNCs 0% and HAX-CNCs 0.5% vs HAX-CNCs (0.125−0.375%); one symbol $p < 0.05$, two symbols $p < 0.01$, and three symbols $p < 0.001$ by Two-Way ANOVA followed by Tukey posthoc test for multiple comparisons. (B) Digital photographs of the hydrogels before immersion in PBS, after 3 and 9 days of swelling (from left to right).

DOI: 10.1021/acs.bioconjchem.5b00209
Bioconjugate Chem. 2015, 26, 1571−1581

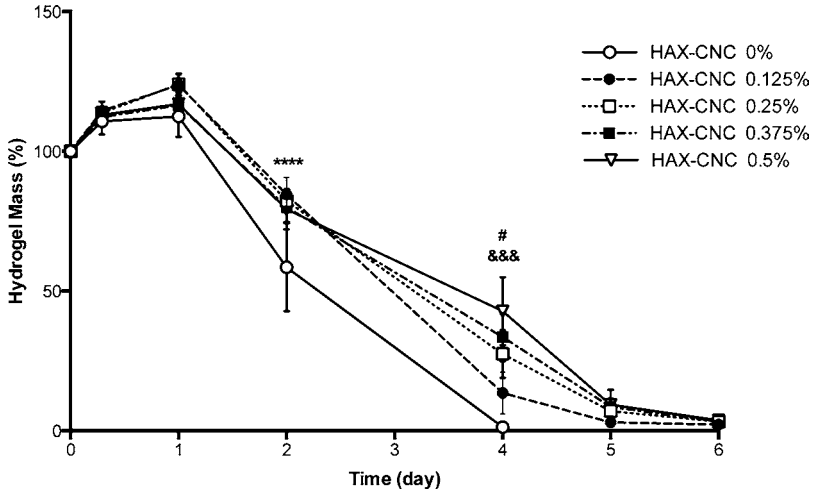

Figure 6. Degradation profile of the hydrogels in 10 U/mL hyaluronidase in PBS at 37 °C. * HAX-CNC 0% vs all other groups, # HAX-CNC 0.125% vs all other groups, & HAX-CNC 0.25% vs HAX-CNC 0.5%; one symbol $p < 0.05$, three symbols $p < 0.001$, and four symbols $p < 0.0001$ by Two-Way ANOVA followed by Tukey posthoc test for multiple comparisons.

hydrogels. At this point in time, remaining formulations were still swelling, and after 6 days HAX-CNC (0.25−0.375%) hydrogels also reached the equilibrium presenting a mass increase of 85 ± 8.9% and 76 ± 7.1%, respectively. Bare HAX hydrogels and with 0.125 wt % CNCs reached equilibrium within 9 days of incubation period and a mass increase of 98 ± 14.3% and 103 ± 19.6%, respectively. After this point in time, hydrogels without CNCs started undergoing hydrolytic degradation while the remaining samples' weight remained approximately unaltered for the completion of the experiment. The swelling profile of hydrogels largely depends on the hydrophilic ability of its functional groups and the cross-link density.[41] The incorporation of CNCs may reduce the mobility of the hydrogel network chains, due to the formation of more physical and covalent bonding in the hydrogel structure, leading to an increase of the cross-linking density and, ultimately, reducing its swelling ability.[19,41] With the exception of HAX-CNC 0.125% samples, the equilibrium swelling ratio showed a decreasing trend with increasing CNC content in the samples, which may be attributed to the increased degree of network cross-linking. In spite of HAX-CNC 0.125% and HAX-CNC 0% hydrogels presenting a similar swelling behavior, with the former having a slightly higher equilibrium swelling ratio, the lower degree of cross-linking of the hydrogels without CNCs is evidenced by the earlier start of hydrolytic degradation. The shape of the hydrogels was also monitored during the assay (Figure 5B). After 9 days of incubation, the HAX-CNC (0.25−0.5%) hydrogels were able to maintain their shape. Conversely, HAX-CNC (0−0.125%) presented some structure deformation at this time point. The swelling behavior described here is similar to other previously reported studies on HAX[38] as well as other polymereric hydrogels reinforced with CNCs.[19,33,41]

The degradation profile of the hydrogels in the presence of hyaluronidase was monitored as a function of incubation time (Figure 6). All HAX-CNC hydrogels swelled during the first day of incubation. HAX hydrogels without CNCs were found to degrade more rapidly than the other hydrogel formulations. After 2 days of incubation, HAX-CNC 0% presented a mass loss significantly higher than the other samples, being completely dissolved after 4 days. At this point in time, HAX-CNC (0.125−0.5%) hydrogels that were presenting a similar degradation profile started to display a decreasing trend with increasing of CNC content in the hydrogels network. The higher degradation rate of hydrogels with lower CNC content may be related with the increased interactions of the more swelled hydrogels with the enzymatic solution, probably due to the decreased cross-linking density of the network. The degradation behavior reported here is consistent with the data obtained during the assessment of the swelling profile of these samples. The increased equilibrium swelling ratio of HAX-CNC 0% reflects its increased rate of degradation in PBS alone and in PBS with hyaluronidase. The degradation behavior described here is similar to that previously reported by other authors for HA-based hydrogels,[13,39] demonstrating that the incorporation of a-CNCs in the HA matrix does not hamper their in vivo resorbable properties by native environment, but could modulate it to some extent. It should also be emphasized that the hyaluronidase concentration used in the degradation study was 10 U/mL, which is in the upper limit of that found in physiological conditions (ranging from 0.0059 U/mL in human plasma to 38.5 U/mL in human ovaries[13]). Although statistically significant differences were observed among HAX hydrogels filled with different a-CNC contents, these would probably be more evident if lower concentrations of hyaluronidase were used. Thus, the proposed strategy may also be considered a suitable tool to modulate the degradation profile of HAX hydrogels in physiological conditions.

Cellular Interactions with HA-CNCs Hydrogels. The ability of hydrogels to support cell adhesion and proliferation and to control cellular behaviors is essential for tissue engineering applications. The hASCs were selected for this study due to their multipotency and ability to differentiate into various lineages.[42,43] Adipose tissue is an abundant source of autologous adult stem cells, which may be implicated in a variety of cell-based therapies for the regeneration of acute and chronically damaged tissues.[44,45] To ensure that developed injectable hydrogels, reinforced with a-CNCs, have preferential cell supportive properties, we tested the ability of hASCs to adhere on the surface of produced nanocomposites and HAX. The results shown that hASCs seeded on hydrogels with incorporated CNCs were spread onto the surface and exhibited elongated shapes even after 1 day of culturing (Figure 7B,C), while only disparate round-shaped cells were found on the surface of hydrogel samples produced without CNCs (Figure

DOI: 10.1021/acs.bioconjchem.5b00209
Bioconjugate Chem. 2015, 26, 1571−1581

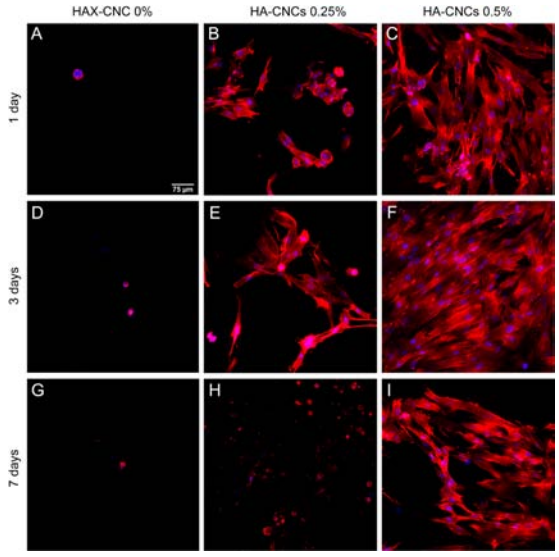

Figure 7. Actin filaments stained with phalloidin (red) and nuclei stained with DAPI (blue) of hASCs seeded onto the surface of HAX-CNC 0% and HAX-CNCs hydrogels after 1 (A–C), 2 (D–F), and 7 (G–I) days of culturing.

7A). The contents of CNCs corresponded with cell density, morphology, and cytoskeleton organization. Cells seeded on HAX-CNC 0.5% hydrogel samples were generally more elongated and spread on the surface with pronounced and extended actin filaments reaching confluence after 3 days of culturing (Figure 7F). At the same time, hASCs cultured on HAX-CNCs 0.25% specimen looked more scattered, and formed clusters in which cells demonstrated spherical appearance and amorphous actin cytoskeleton (Figure 7E). Considering that E' values of both hydrogel compositions incorporating CNCs are on the same order (152 and 127 kPa for 0.25% and 0.5% CNCs content, respectively), the higher density of SO_3^- groups of HAX-CNCs 0.5% may play a significant role on the different adhesion trends observed for these hydrogels. It is known that sulfated GAGs have the ability to noncovalently bind and modulate cytokines, growth factors, and other ECM proteins via electrostatic interactions and enhance cellular activities, such as attachment, proliferation, and migration.[32,46] We hypothesize that CNCs can potentially act as sulfated GAGs mimics. This advantageous functionality has been suggested in a recent study where sulfated CNCs were successfully used to create anticoagulant surface coatings, mimicking the role of heparin.[47] Thus, the incorporation of sulfated CNCs into HAX-CNC 0% may locally amplify biomolecular signals and positively impact the cell–matrix interactions, promoting cellular adhesion and proliferation in a concentration dependent manner.

However, after 7 days we observed a remarkable negative trend in cell supportive properties in both groups of hydrogels reinforced with CNCs. The number of cells attached to the surface of HAX-CNCs hydrogels was significantly decreased. Extant hASCs displayed grossly abnormal morphology or were partially detached and disrupted. The effects described above are more likely caused by loss of integrity and surface erosion accompanied by swelling process of hydrogel samples. It was shown that for adherent fibroblast like cells including hASCs survival depends upon anchorage onto an integer surface. The loss of anchorage-dependent attachment to the matrix leads to the form of programmed cell death known as "anoikis".[48,49] Thus, erosion of hydrogel surfaces on the later experimental time point (7 days) adversely affected adhesive properties of substrate and constrain normal cell growth and behavior. Nevertheless, a large number of hASCs cultured on HAX-CNC 0.5% hydrogels have retained the ability to adhere and maintain normal morphology (Figure 7I) in contrast with cells cultured HAX-CNCs 0.25% (Figure 7H). This behavior correlates well with the swelling and degradation profiles of the different hydrogel formulations described in previous sections. The swelling ratio was significantly higher and the degradation in the presence of hyaluronidase was faster for HAX-CNC 0% than for the hydrogels incorporating CNCs in a concentration dependent manner. HAX-CNCs 0.5% swelled less and offer higher resistance to enzymatic degradation compared to HAX-CNCs 0.25%.

To examine the capability of developed nanocomposites to entrap cells and to control cellular behavior we evaluated DNA content, metabolic activity, and viability of encapsulated hASCs after 1, 3, and 7 days of culturing. The hASCs remained viable

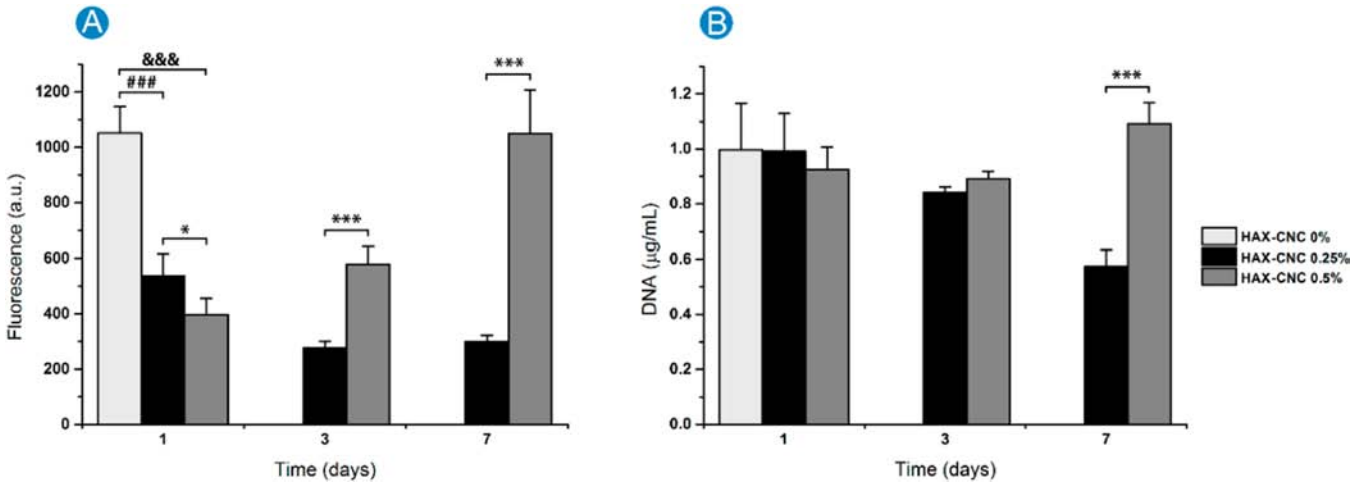

Figure 8. Mitochondrial activity (A) and DNA content (B) of encapsulated hASCs (4×10^5 cells/hydrogel) assessed by the Alamar Blue and PicoGreen assays, respectively. * HAX-CNC 0.25% vs HAX-CNC 0.5%, # HAX-CNC 0% vs HAX-CNC 0.25%, & HAX-CNC 0% vs HAX-CNC 0.5%; one symbol $p < 0.05$, three symbols $p < 0.0001$ by Two-Way ANOVA followed by Tukey posthoc test for multiple comparisons.

DOI: 10.1021/acs.bioconjchem.5b00209
Bioconjugate Chem. 2015, 26, 1571–1581

after encapsulation in all hydrogels under study after initial time point (1 days), as evident by the metabolic activity and Live/Dead staining. Alamar Blue assay was used to evaluate the mitochondrial activity of the cells cultured inside the nanocomposites. Interestingly, the hASCs entrapped in HAX-CNC 0% hydrogel samples demonstrated higher metabolic activity after 1 day of culturing (Figure 8A), whereas DNA contents remained nearly identical in all experimental groups (HAX-CNC 0%, HAX-CNCs 0.25%, and HAX-CNCs 0.5%) (Figure 8B). The observed effect may be associated with differences in microstructure, swelling, and mechanical properties of the hydrogels. Being softer and exhibiting a lower cross-linking density, HAX-CNC 0% initially facilitated faster nutrient diffusion and matrix remodeling, thus promoting cellular activities such as spreading and migration, as previously reported on other studies,[50,51] explaining the higher cellular metabolic activity observed in these hydrogels.

Results of Live/Dead staining support this hypothesis, revealing the presence of cells on the initial phase of spreading in hydrogels without CNCs after 1 day of culturing (Figure 9A), while cells in hydrogels formed with CNCs maintained

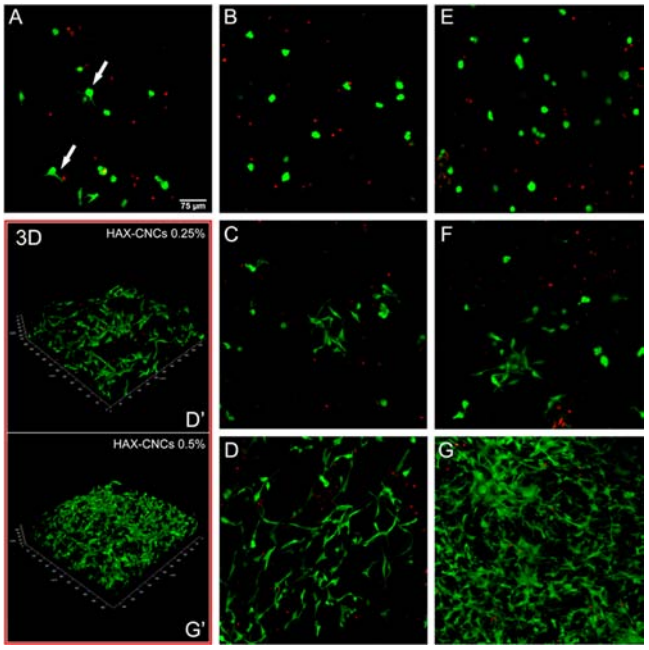

Figure 9. Live/Dead staining with Calcein AM/PI (green: live cell; red: dead cell) of hASCs encapsulated in (A) HAX-CNC 0% hydrogels after 1 day, spread cells marked with white arrows; HAX-CNCs 0.25% hydrogels after 1 (B), 3 (C), and 7 (D) days; HAX-CNCs 0.5% hydrogels after 1 (E), 3 (F), and 7 (G) days after encapsulation. 3D reconstruction based on confocal imaging of HAX-CNCs 0.25% - *D′* and HAX-CNCs 0.5% - *G′* hydrogels, 7 days after encapsulation (120 μm *z*-stack).

spherical shape (Figure 9B and E). Cell spreading inside hydrogels required the displacement or degradation of the polymer matrix in order to create suitable microdomains for their movement. Thus, lower degree of cross-linking in HAX-CNC 0% hydrogels provided hASCs freedom to spread and potentially increased their metabolic activity on early experimental time points. However, fast degradation of HAX-CNC 0% hydrogel samples did not allow us to assess metabolic activity or DNA contents on later time points. The hydrogels formed without CNCs were found to be completely dissolved after 2 days of culture. On the later experimental time points (3 and 7 days) hASCs encapsulated in HAX-CNCs 0.25% and HAX-CNCs 0.5% samples exhibited spindle-like morphology and extensive spreading (Figure 9C and F). We detected that this type of cell behavior was more pronounced in hydrogels formed with 0.5% then 0.25% of CNCs especially after 7 days of culturing (Figure 9D and G). Moreover, 3D reconstruction based on confocal imaging showed the presence of well-developed multidimensional networks of cell-to-cell and cell–matrix contacts (Figure 9D′ and *G′*) that can be considered an early indicator of the formation of functionally integrated tissue-like structure.[52] This finding is also in agreement with quantitative evaluation of DNA content and metabolic activity. From the DNA assay data, it was possible to confirm that after 7 days of culture the different concentrations of CNCs in hydrogels induced significant changes in the hASCs content (Figure 8B). The metabolic activity rate of cells in HAX-CNCs 0.25% hydrogels was also significantly lower than the rates for HAX-CNCs 0.25% hydrogels after 3 and 7 days of culturing (Figure 8A). The decreased DNA concentration and metabolic activity observed for HAX-CNCs 0.25% could be partially related to the hydrogel degradation dependent cell release that was noted during collection of samples (data not shown). Taking together, obtained results clearly demonstrate that the concentration of CNCs in nanocomposites directly correlates with cell supportive properties of the developed injectable HAX-CNCs hydrogels.

CONCLUSIONS

In this work we propose a biobased strategy for the development of injectable HA-based nanocomposite hydrogels with improved structural, mechanical, and degradation performance. The developed hydrogels, composed of in situ cross-linkable ADH-HA and a-HA, were reinforced with variable amounts of a-CNCs that can act as multifunctional cross-linker through physical interactions and covalent bonding with the HA matrix. The gelation times of all the hydrogel formulations were very similar and occurred within the range of 15–17 s. Moreover, the incorporation of a-CNCs into the HA matrix resulted in a more organized and compacted network with significantly smaller pore sizes, and led to stiffer hydrogels with a storage modulus up to 2.7-fold higher than that of unfilled hydrogels. Results from swelling and enzymatic degradation showed that increased amounts of a-CNCs led, in general, to lower equilibrium swelling ratios and higher resistance to degradation. These results, combined with the fact that these bionanocomposite hydrogels can be prepared in a liquid form and easily extruded using a double-barrel syringe, may represent a useful tool to broaden the potential range of applications of hyaluronic acid-based hydrogels in the field of TE. HAX-CNC hydrogels demonstrated enhanced adhesive properties with seeded hASCs. The cells were spread onto the surface and exhibited typical elongated morphology while only disparate round-shaped cells were found on the surface of HAX hydrogels. The examination of biological performances of HAX-CNCs with encapsulated hASCs hydrogels clearly demonstrated that the concentration of CNCs in nanocomposites directly correlates with cell supportive properties, such as viability, metabolic activity, and proliferation rate. Overall, the HAX-CNCs nanocomposites were shown to combine preferable mechanical and stability properties with mimetic ECM biochemical cues which can significantly impact their biological performance in TE applications.

DOI: 10.1021/acs.bioconjchem.5b00209
Bioconjugate Chem. 2015, 26, 1571–1581

EXPERIMENTAL SECTION

Materials. Microcrystalline cellulose powder (MCC), sodium periodate ($NaIO_4$), potassium bromide (KBr), silver(I) oxide, ethylene glycol, adipic dihydrazide (ADH), 1-[3-(dimethylamino)propyl]-3-ethylcarbodiimide hydrochloride (EDC), *tert*-butyl carbazate (*t*BC), sodium cyanoborohydride, sodium acetate, acetic acid, hyaluronidase, and phosphate buffered saline were purchased from Sigma-Aldrich. Sodium hyaluronate (HA; M_w = 253 kDa) research grade was purchased from Lifecore Biomedical, USA. Sodium hydroxide and hydrochloric acid were purchased from VWR, France. Concentrated sulfuric acid (95−98%) was purchased from Laborspirit, Portugal.

Preparation of CNC and CNC Oxidation. Cellulose nanocrystals (CNC) were extracted from microcrystalline cellulose powder (MCC) following the typical sulfuric acid hydrolysis according to Bondeson et al.[53] The concentration of CNC was determined gravimetrically to be of 1.5 wt % in a yield of 31.5 wt %. Aldehyde functionalized CNCs (a-CNC) were produced by sodium periodate oxidation as described elsewhere[33] with minor adaptations. The a-CNC concentration was determined gravimetrically to be 1.4 wt %. For detailed experimental procedures and characterizations of CNC and a-CNC, see Supporting Information.

Hydrazide Functionalization and Aldehyde-Modification of HA. Hydrazide-modified HA (HA-ADH) was produced following previously established carbodiimide chemistry,[13,17,54] as depicted in Figure S5, giving a degree of substitution of 24.3 ± 2%. Synthesis of a-HA was performed by sodium periodate ($NaIO_4$) oxidation, as described elsewhere, with slight modifications,[6] resulting in a degree of oxidation of 4.5%. For details on the synthesis and characterization of HA derivatives, see Supporting Information.

Preparation of Injectable Hydrogel and Hydrogel Nanocomposites. The hydrogels were prepared at room temperature by mixing equal amounts of aldehyde and hydrazide derivatives of hyaluronic acid (see Figure 1). A double-barrel syringe, fitted with a static mixer placed at the outlet (L-System, Medmix, Switzerland) and a gauge needle (18 G) fitted to the mixer tip, was used to produce injectable hydrogels of covalently cross-linked HA (HAX) and HAX-CNCs. For HAX, each component was dissolved in ultrapure water (2% w/v solution). Barrel A was filled with HA-ADH and barrel B with a-HA. The hydrogel precursor solutions were then hand extruded into cylindrical Teflon molds (5 mm in diameter × 5 mm in height). HAX-CNCs nanocomposite hydrogels were prepared following similar procedures but dissolving a-HA (2% w/v) in a-CNCs water dispersions at 0.25, 0.5, 0.75, and 1 wt % concentration, prepared from dilutions of the original 1.39 wt % a-CNCs suspensions. Before extrusion, the a-HA/a-CNCs solutions were briefly sonicated (3 pulses of 10 s) to ensure uniform suspension. The final hydrogels were composed of 1 wt % HA-ADH, 1 wt % a-HA, and 0.125 to 0.5 wt % a-CNC.

Fourier Transform Infrared Spectroscopy (FTIR). Freeze-dried CNCs, a-CNCs, a-HA, and HA-ADH and HAX samples were oven-dried at 105 °C for 3 h and then cooled to room temperature preventing air exposure to avoid water resorption before FT-IR analysis. The samples were pressed into KBr pellets, and FT-IR spectra were collected with IRPrestige 21 FTIR spectrophotometer (Shimadzu). Spectra were obtained in the 400−4000 cm^{-1} range and for each sample 32 scans were taken at a resolution of 4 cm^{-1}.

Scanning Electron Microscopy (SEM). Morphology of the freeze-dried HAX hydrogels was observed by scanning electron microscopy (SEM) (JSM-6010LV, JEOL, Japan). For this purpose, the hydrogels were quickly frozen using liquid nitrogen in order to minimize the processing impact on the samples' network structure and then freeze-dried for 4 days. The freeze-dried gels were fractured after cooling in liquid nitrogen to expose their inner structures, and the fractured sample was sputter coated (30 s at 20 mA, Cressington) with gold prior to observation.

Dynamic Mechanical Analysis (DMA). The viscoelastic measurements were performed using a TRITEC 2000 DMA from Triton Technology (UK), equipped with the compressive mode. The measurements were carried out at room temperature (RT). All the hydrogels were cylindrical with a diameter of ∼5 mm and a thickness of ∼5 mm (measured accurately for each sample). Hydrogels were always analyzed immersed in a liquid bath placed in a Teflon reservoir. Samples were previously immersed in a PBS solution for 24 h to reach equivalent swelling. The dimensions of the samples were then measured and the samples were clamped in the DMA apparatus and immersed in the PBS solution. DMA spectra were obtained during a frequency scan between 0.5 and 10 Hz. The experiments were performed under constant strain amplitude (50 μm). At least three different hydrogels were tested for each composition with the same experimental settings and the presented data represent average values.

In Situ Gelation Time of the Hydrogels. The apparent in situ gelation time of the hydrogel was measured at room temperature as previously described[13] (see Movie in Supporting Information). A magnetic stirring bar was placed in the center of a 100 μL droplet of HA-ADH aqueous solution (2 wt %) in a Petri dish and stirred at 160 rpm using a magnetic stirrer. 100 μL of a-HA or a-HA/a-CNC solutions (2 wt % HA, 0−1 wt % a-CNCs) was then added to the HA-ADH drop while stirring and the apparent gelation time was recorded when the solution formed a solid globule (n = 4).

Swelling and Degradation. The prepared hydrogels were initially weighed (W_0), immersed in PBS, and kept at 37 °C for 20 days. At each time point the immersed hydrogels were removed and immediately weighed (W_f), after the excess of water was absorbed with a filter paper. The swelling ratio was calculated using the following equation:

$$\text{Swelling ratio } (\%) = \frac{W_f - W_i}{W_i} \times 100 \quad (1)$$

The assay proceeded after the swelling equilibrium was reached in order to assess the degradation kinetics of the swollen hydrogels in PBS.

For assessing the enzymatic degradation profile, the hydrogels were first incubated in PBS at 37 °C for 2 h. After this period, the hydrogels were weighed (W_i) and subsequently incubated in 2 mL of PBS with 10 U/mL hyaluronidase at 37 °C,[39] under constant agitation in a horizontal orbital shaker at 180 rpm. At each preselected time point (6 h and 1, 2, 4, 5, 6 days), the hydrogels were weighed (W_f), and the enzymatic solution was replaced. Measurements were performed until complete degradation of the samples. The degradation was calculated using the following equation:

DOI: 10.1021/acs.bioconjchem.5b00209
Bioconjugate Chem. 2015, 26, 1571−1581

$$\text{Hydrogel Mass}\ (\%) = \frac{W_f}{W_i} \times 100 \quad (2)$$

Hydrogels were photographed at several time-points.

Human Adipose-Derived Stem Cells Isolation and Expansion. Human adipose tissue derived mesenchymal stem cells (hASCs) were obtained from lipo-aspirate samples of the abdominal region of patients undergoing plastic surgery, under the scope of previously established protocols with Hospital da Prelada (Porto, Portugal). All related procedures were approved by the Hospital Ethics Committee. The hASCs were isolated from the adipose tissue specimens and cultured as described before.[55] Briefly, the tissue was rinsed with PBS (Sigma-Aldrich) containing 10% of an antibiotic−antimycotic solution (A/A, Alfagene, USA). The fatty fraction was incubated in a 0.05% collagenase type II (Sigma/C6885) solution for 60 min with gentle agitation at 37 °C. Digested tissue was centrifuged at 800 *g* for 10 min at 4 °C to remove supernatant. Primary culture of hASCs was expanded in basic media a-MEM (Gibco, UK) supplemented with 10% FBS (Alfagene, USA), and 1% A/A solution (Alfagene, USA) at 37 °C, 5% CO_2.

Encapsulation of hASCs in HA-CNCs Hydrogels and in Vitro Cell Culture. Cultured hASCs were detached by trypsin and centrifuged at 350 *g* for 5 min. The obtained cell pellet was resuspended in sterile PBS solution, counted using a hemocytometer and finally centrifuged. The supernatant was discarded and HA-ADH solution was added to the cells to obtain a final concentration of 4×10^6 cells/mL. The cell suspension was thoroughly mixed to homogenize the distribution of the cells within the matrix. Hydrogel samples containing hASCs were prepared under sterile conditions using a cylindrical mold (5.0 ± 0.1 mm diameter and 5.0 ± 0.1 mm height) and incubated at room temperature for 20 min to form a solid gel. The hydrogels with encapsulated cells were cultured in 48 well plates in basal media for 1, 3, and 7 days (37 °C, 5% CO_2) with the culture media replaced after 3 days.

Cell-Seeded HA-CNCs Hydrogels. Cultured hASCs were initially treated as described in the previous section and then resuspended in 150 μL of basal culture media and seeded on the surface of hydrogel samples (9.0 ± 0.1 mm diameter and 2.0 ± 0.1 mm height) at a concentration of 4×10^4 cells/sample. Seeded hydrogels were incubated (37 °C, 5% CO_2) for 1 h to allow initial cell attachment before the addition of the culture media to the wells. The cell-seeded hydrogels were cultured in 24 well plates in basal media for 1, 3, and 7 days (37 °C, 5% CO_2) with the culture media replacement after 3 days.

Cell Viability and Metabolic Activity Assessment. At the end of each time point of the study, the HA-CNCs hydrogel samples with encapsulated hASCs were placed in new 48 well culture plates, incubated with Calcein AM (Invitrogen, USA) 1:1000 v/v and propidium iodide (PI, AlfaGen, USA) 1:1000 v/v solution in PBS for 30 min at 37 °C and washed in PBS to reduce background fluorescence. Processed samples were mounted on microscopic slides and visualized by confocal microscope TCS SP8 (Leica Microsystems, Germany).

The Alamar Blue (Bio-Rad, England) fluorescent assay was used to assess the metabolic activity of encapsulated cells. At each pre-settled time point, the culture medium was aspirated and samples were rinsed with PBS and incubated with 750 μL of 10% v/v Alamar Blue in a basal culture media solution for 4 h at 37 °C, 5% CO_2. Then, the 200 mL aliquots of the mixture were transferred to a 96 well plate. The fluorescence of Alamar Blue was measured using a Synergy HT microplate reader (Bio-Tek, USA) at excitation and emission wavelength of 530 and 590 nm, respectively.

Cell Morphology and Cytoskeleton Organization. To investigate the ability of developed hydrogels to support the cell adhesion, the structure of actin filaments in hASCs seeded on the surface of nanocomposites was examined after 1, 3, and 7 days of culture. For this purpose, the samples were rinsed twice with PBS and then fixed in 10% formalin (Enzifarma, Portugal) for 30 min at room temperature. After three washes in PBS, fixed samples were incubated with rhodamine-conjugated phalloidin (Sigma-Aldrich, USA) 1:500 v/v and 4′,6-diamidino-2-phenylindole (DAPI, Sigma-Aldrich, USA) 1:1000 v/v solution in PBS for 30 min at room temperature. After rinsing in PBS, processed hydrogel samples were mounted onto coverslips and finally observed under a confocal microscope TCS SP8 (Leica Microsystems, Germany).

Statistical Analysis. The statistical analysis of data was performed using GraphPad PRISM v 6.0. The experimental data from pore size measurements, swelling, and degradation behavior were analyzed using one-way or two-way analysis of variance (ANOVA), followed by Tukey posthoc test for multiple comparisons. Statistical significance was set to $p < 0.05$. Results are presented as mean ± standard deviation.

■ ASSOCIATED CONTENT

Supporting Information

Morphological and chemical characterization of CNC and a-CNC, S2; characterization of HA derivatives, S6; methods, S9; experiment of apparent gelation time movie. The Supporting Information is available free of charge on the ACS Publications website at DOI: 10.1021/acs.bioconjchem.5b00209.

■ AUTHOR INFORMATION

Corresponding Author

*E-mail: megomes@dep.uminho.pt. Tel.: +351253510906.

Notes

The authors declare no competing financial interest.

■ ACKNOWLEDGMENTS

The authors acknowledge Dr. Igor Bdikin of Department of Mechanical Engineering, Centre for Mechanical Technology & Automation, University of Aveiro, for the XRD acquisition, and Dr. Ramon Novoa-Carballal and Dr. Carla Silva for the GPC analysis. The authors also acknowledge the financial support from the Project RL1 - ABMR - NORTE-01-0124-FEDER-000016 cofinanced by North Portugal Regional Operational Programme (ON.2 − O Novo Norte), under the National Strategic Reference Framework (NSRF), through the European Regional Development Fund (ERDF).

■ REFERENCES

(1) Fraser, J. R. E., Laurent, T. C., and Laurent, U. B. G. (1997) Hyaluronan: Its nature, distribution, functions and turnover. *J. Intern. Med. 242*, 27−33.

(2) Jiang, D., Liang, J., and Noble, P. W. (2007) Hyaluronan in Tissue Injury and Repair. *Annu. Rev. Cell Dev. Biol. 23*, 435−461.

(3) Sahoo, S., Chung, C., Khetan, S., and Burdick, J. A. (2008) Hydrolytically Degradable Hyaluronic Acid Hydrogels with Controlled Temporal Structures. *Biomacromolecules 9*, 1088−1092.

(4) Toole, B. P. (2004) Hyaluronan: from extracellular glue to pericellular cue. *Nat. Rev. Cancer 4*, 528−39.

DOI: 10.1021/acs.bioconjchem.5b00209
Bioconjugate Chem. 2015, 26, 1571−1581

(5) Burdick, J. A., and Prestwich, G. D. (2011) Hyaluronic acid hydrogels for biomedical applications. *Adv. Mater. 23*, H41−56.
(6) Tan, H., Chu, C. R., Payne, K. A., and Marra, K. G. (2009) Injectable in situ forming biodegradable chitosan-hyaluronic acid based hydrogels for cartilage tissue engineering. *Biomaterials 30*, 2499−506.
(7) Menzel, E. J., and Farr, C. (1998) Hyaluronidase and its substrate hyaluronan: biochemistry, biological activities and therapeutic uses. *Cancer Lett. 131*, 3−11.
(8) Chen, J.-P., and Cheng, T.-H. (2009) Preparation and evaluation of thermo-reversible copolymer hydrogels containing chitosan and hyaluronic acid as injectable cell carriers. *Polymer 50*, 107−116.
(9) Su, W. Y., Chen, Y. C., and Lin, F. H. (2010) Injectable oxidized hyaluronic acid/adipic acid dihydrazide hydrogel for nucleus pulposus regeneration. *Acta Biomater. 6*, 3044−55.
(10) Bae, K. H., Wang, L.-S., and Kurisawa, M. (2013) Injectable biodegradable hydrogels: progress and challenges. *J. Mater. Chem. B 1*, 5371.
(11) Burdick, J. A., Chung, C., Jia, X., Randolph, M. A., and Langer, R. (2005) Controlled Degradation and Mechanical Behavior of Photopolymerized Hyaluronic Acid Networks. *Biomacromolecules 6*, 386−391.
(12) Li, Y., Rodrigues, J., and Tomas, H. (2012) Injectable and biodegradable hydrogels: gelation, biodegradation and biomedical applications. *Chem. Soc. Rev. 41*, 2193−221.
(13) Yeo, Y., Highley, C. B., Bellas, E., Ito, T., Marini, R., Langer, R., and Kohane, D. S. (2006) In situ cross-linkable hyaluronic acid hydrogels prevent post-operative abdominal adhesions in a rabbit model. *Biomaterials 27*, 4698−4705.
(14) Alves, M. H., Young, C. J., Bozzetto, K., Poole-Warren, L. A., and Martens, P. J. (2012) Degradable, click poly(vinyl alcohol) hydrogels: characterization of degradation and cellular compatibility. *Biomed. Mater. 7*, 024106.
(15) Bulpitt, P., and Aeschlimann, D. (1999) New strategy for chemical modification of hyaluronic acid: Preparation of functionalized derivatives and their use in the formation of novel biocompatible hydrogels. *J. Biomed. Mater. Res. 47*, 152−169.
(16) Maia, J., Ferreira, L., Carvalho, R., Ramos, M. A., and Gil, M. H. (2005) Synthesis and characterization of new injectable and degradable dextran-based hydrogels. *Polymer 46*, 9604−9614.
(17) Dahlmann, J., Krause, A., Möller, L., Kensah, G., Möwes, M., Diekmann, A., Martin, U., Kirschning, A., Gruh, I., and Dräger, G. (2013) Fully defined in situ cross-linkable alginate and hyaluronic acid hydrogels for myocardial tissue engineering. *Biomaterials 34*, 940−951.
(18) Gurski, L. A., Jha, A. K., Zhang, C., Jia, X., and Farach-Carson, M. C. (2009) Hyaluronic acid-based hydrogels as 3D matrices for in vitro evaluation of chemotherapeutic drugs using poorly adherent prostate cancer cells. *Biomaterials 30*, 6076−6085.
(19) Yang, X., Bakaic, E., Hoare, T., and Cranston, E. D. (2013) Injectable Polysaccharide Hydrogels Reinforced with Cellulose Nanocrystals: Morphology, Rheology, Degradation, and Cytotoxicity. *Biomacromolecules 14*, 4447−4455.
(20) Zhu, J., and Marchant, R. E. (2011) Design properties of hydrogel tissue-engineering scaffolds. *Expert Rev. Med. Devices 8*, 607−26.
(21) Bhattacharyya, S., Guillot, S., Dabboue, H., Tranchant, J. F., and Salvetat, J. P. (2008) Carbon nanotubes as structural nanofibers for hyaluronic acid hydrogel scaffolds. *Biomacromolecules 9*, 505−509.
(22) Jeon, O., Song, S. J., Lee, K.-J., Park, M. H., Lee, S.-H., Hahn, S. K., Kim, S., and Kim, B.-S. (2007) Mechanical properties and degradation behaviors of hyaluronic acid hydrogels cross-linked at various cross-linking densities. *Carbohydr. Polym. 70*, 251−257.
(23) Collins, M. N., and Birkinshaw, C. (2008) Physical properties of crosslinked hyaluronic acid hydrogels. *J. Mater. Sci.: Mater. Med. 19*, 3335−43.
(24) Habibi, Y., Lucia, L. A., and Rojas, O. J. (2010) Cellulose Nanocrystals: Chemistry, Self-Assembly, and Applications. *Chem. Rev. 110*, 3479−3500.
(25) Moon, R. J., Martini, A., Nairn, J., Simonsen, J., and Youngblood, J. (2011) Cellulose nanomaterials review: structure, properties and nanocomposites. *Chem. Soc. Rev. 40*, 3941−3994.
(26) Lin, N., Huang, J., and Dufresne, A. (2012) Preparation, properties and applications of polysaccharide nanocrystals in advanced functional nanomaterials: a review. *Nanoscale 4*, 3274−3294.
(27) Dri, F., Hector, L., Jr., Moon, R., and Zavattieri, P. (2013) Anisotropy of the elastic properties of crystalline cellulose Iβ from first principles density functional theory with Van der Waals interactions. *Cellulose 20*, 2703−2718.
(28) Rusli, R., and Eichhorn, S. J. (2008) Determination of the stiffness of cellulose nanowhiskers and the fiber-matrix interface in a nanocomposite using Raman spectroscopy. *Appl. Phys. Lett. 93*, 033111.
(29) Šturcová, A., Davies, G. R., and Eichhorn, S. J. (2005) Elastic Modulus and Stress-Transfer Properties of Tunicate Cellulose Whiskers. *Biomacromolecules 6*, 1055−1061.
(30) Domingues, R. M. A., Gomes, M. E., and Reis, R. L. (2014) The Potential of Cellulose Nanocrystals in Tissue Engineering Strategies. *Biomacromolecules 15*, 2327−2346.
(31) Habibi, Y. (2014) Key advances in the chemical modification of nanocelluloses. *Chem. Soc. Rev. 43*, 1519−1542.
(32) Salbach, J., Rachner, T., Rauner, M., Hempel, U., Anderegg, U., Franz, S., Simon, J.-C., and Hofbauer, L. (2012) Regenerative potential of glycosaminoglycans for skin and bone. *J. Mol. Med. 90*, 625−635.
(33) Dash, R., Foston, M., and Ragauskas, A. J. (2013) Improving the mechanical and thermal properties of gelatin hydrogels cross-linked by cellulose nanowhiskers. *Carbohydr. Polym. 91*, 638−645.
(34) Abitbol, T., Johnstone, T., Quinn, T. M., and Gray, D. G. (2011) Reinforcement with cellulose nanocrystals of poly(vinyl alcohol) hydrogels prepared by cyclic freezing and thawing. *Soft Matter 7*, 2373−2379.
(35) Han, J., Lei, T., and Wu, Q. (2014) High-water-content mouldable polyvinyl alcohol-borax hydrogels reinforced by well-dispersed cellulose nanoparticles: dynamic rheological properties and hydrogel formation mechanism. *Carbohydr. Polym. 102*, 306−316.
(36) Zhang, X., Huang, J., Chang, P. R., Li, J., Chen, Y., Wang, D., Yu, J., and Chen, J. (2010) Structure and properties of polysaccharide nanocrystal-doped supramolecular hydrogels based on Cyclodextrin inclusion. *Polymer 51*, 4398−4407.
(37) Kim, U.-J., Kuga, S., Wada, M., Okano, T., and Kondo, T. (2000) Periodate Oxidation of Crystalline Cellulose. *Biomacromolecules 1*, 488−492.
(38) Ossipov, D. A., Piskounova, S., Varghese, O. P., and Hilborn, J. (2010) Functionalization of Hyaluronic Acid with Chemoselective Groups via a Disulfide-Based Protection Strategy for In Situ Formation of Mechanically Stable Hydrogels. *Biomacromolecules 11*, 2247−2254.
(39) Ito, T., Yeo, Y., Highley, C. B., Bellas, E., Benitez, C. A., and Kohane, D. S. (2007) The prevention of peritoneal adhesions by in situ cross-linking hydrogels of hyaluronic acid and cellulose derivatives. *Biomaterials 28*, 975−83.
(40) DeForest, C. A., and Anseth, K. S. (2012) Advances in Bioactive Hydrogels to Probe and Direct Cell Fate. *Annu. Rev. Chem. Biomol. Eng. 3*, 421−444.
(41) Zhou, C., Wu, Q., Yue, Y., and Zhang, Q. (2011) Application of rod-shaped cellulose nanocrystals in polyacrylamide hydrogels. *J. Colloid Interface Sci. 353*, 116−123.
(42) Zuk, P. A., Zhu, M., Mizuno, H., Huang, J., Futrell, J. W., Katz, A. J., Benhaim, P., Lorenz, H. P., and Hedrick, M. H. (2001) Multilineage cells from human adipose tissue: Implications for cell-based therapies. *Tissue Eng. 7*, 211−228.
(43) Gimble, J. M., and Guilak, F. (2003) Adipose-derived adult stem cells: Isolation, characterization, and differentiation potential. *Cytotherapy 5*, 362−369.
(44) Pikuła, M., Marek-Trzonkowska, N., Wardowska, A., Renkielska, A., and Trzonkowski, P. (2013) Adipose tissue-derived stem cells in clinical applications. *Expert Opin. Biol. Ther. 13*, 1357−1370.
(45) Lauritano, D., Palmieri, A., Vinci, R., Azzi, L., Taglabue, A., and Carinci, F. (2014) Adipose derived stem cells: basic science

DOI: 10.1021/acs.bioconjchem.5b00209
Bioconjugate Chem. 2015, 26, 1571−1581

fundaments and clinical application. An update. *Minerva Stomatol. 63*, 273−281.
(46) Hortensius, R. A., and Harley, B. A. C. (2013) The use of bioinspired alterations in the glycosaminoglycan content of collagen−GAG scaffolds to regulate cell activity. *Biomaterials 34*, 7645−7652.
(47) Ehmann, H. M. A., Mohan, T., Koshanskaya, M., Scheicher, S., Breitwieser, D., Ribitsch, V., Stana-Kleinschek, K., and Spirk, S. (2014) Design of anticoagulant surfaces based on cellulose nanocrystals. *Chem. Commun. 50*, 13070−13072.
(48) Frisch, S. M., and Francis, H. (1994) Disruption of epithelial cell-matrix interactions induces apoptosis. *J. Cell Biol. 124*, 619−626.
(49) Lee, S., Choi, E., Cha, M. J., and Hwang, K. C. (2015) Cell adhesion and long-term survival of transplanted mesenchymal stem cells: A prerequisite for cell therapy. *Oxid. Med. Cell. Longevity 2015*, 110.1155/2015/632902
(50) Lei, Y., Gojgini, S., Lam, J., and Segura, T. (2011) The spreading, migration and proliferation of mouse mesenchymal stem cells cultured inside hyaluronic acid hydrogels. *Biomaterials 32*, 39−47.
(51) Lee, H.-J., Sen, A., Bae, S., Lee, J. S., and Webb, K. (2015) Poly(ethylene glycol) diacrylate/hyaluronic acid semi-interpenetrating network compositions for 3-D cell spreading and migration. *Acta Biomater. 14*, 43−52.
(52) Rosso, F., Giordano, A., Barbarisi, M., and Barbarisi, A. (2004) From Cell-ECM Interactions to Tissue Engineering. *J. Cell. Physiol. 199*, 174−180.
(53) Bondeson, D., Mathew, A., and Oksman, K. (2006) Optimization of the isolation of nanocrystals from microcrystalline cellulose by acid hydrolysis. *Cellulose 13*, 171−180.
(54) Vercruysse, K. P., Marecak, D. M., Marecek, J. F., and Prestwich, G. D. (1997) Synthesis and in vitro degradation of new polyvalent hydrazide cross-linked hydrogels of hyaluronic acid. *Bioconjugate Chem. 8*, 686−94.
(55) Rada, T., Reis, R. L., and Gomes, M. E. (2011) Distinct stem cells subpopulations isolated from human adipose tissue exhibit different chondrogenic and osteogenic differentiation potential. *Stem Cell Rev. 7*, 64−76.

DOI: 10.1021/acs.bioconjchem.5b00209
Bioconjugate Chem. 2015, 26, 1571−1581